

CHAPTER 6

Ferrofluid Lubrication of a Long Journal Bearing with Transverse Magnetic Field

CONTENTS

Symbols

6.1 Introduction

6.2 Analysis

6.3 Static Performance

6.3.1 Calculation of bearing Characteristics

6.4 Dynamic Performance

6.4.1 Calculation of the dimensionless stiffness matrix K and damping matrix C

6.5 Results and Discussion

6.6 Conclusions

References

SYMBOLS

c	radial clearance (m)
C	dimensionless damping matrix defined in equation (6.54)
$C_{R_1R_1}$	dimensionless radial principal damping
$C_{T_1T_1}$	dimensionless tangential principal damping
$C_{R_1T_1}, C_{T_1R_1}$	dimensionless cross-coupled damping coefficients
D_J	journal diameter (m)
e	eccentricity
f_R	dimensionless radial component of fluid film force defined in equation (6.36) for static case
f_{R_1}	dimensionless radial component of fluid film force defined in equation (6.51) for dynamic case
f_T	dimensionless tangential component of fluid film force defined in equation (6.37) for static case
f_{T_1}	dimensionless tangential component of fluid film force defined in equation (6.52) for dynamic case
\bar{f}	dimensionless coefficient of friction on the journal defined in equation (6.42)
F	frictional force on the journal defined in equation (6.40) (N)
FF	ferrofluid
\bar{F}	dimensionless frictional force on the journal defined in equation (6.41)
h	film thickness (m)
$\frac{\partial h}{\partial t}$	squeeze velocity of the journal, (m s^{-1})
H	dimensionless film thickness defined in equation (6.22)

H	magnetic field vector
$ \mathbf{H} $	magnetic field strength (magnitude of H) (A m^{-1})
I	sum of moments of inertia of the particles per unit volume ($\text{N s}^2 \text{m}^{-2}$)
k_B	Boltzmann's constant ($\text{J }(^{\circ}\text{K})^{-1}$)
K	dimensionless stiffness matrix defined in equation (6.53)
$K_{R_1R_1}$	dimensionless radial principal stiffness
$K_{T_1T_1}$	dimensionless tangential principal stiffness
$K_{R_1T_1}, K_{T_1R_1}$	dimensionless cross-coupled stiffness coefficients
$\hat{\mathbf{i}}, \hat{\mathbf{j}}, \hat{\mathbf{k}}$	unit vectors along the x, y, z – axis, respectively
L	length of the bearing in the y – direction (m)
m	magnetic moment of a particle (A m^2)
M	magnetization vector
M_0	equilibrium magnetization (A m^{-1})
MF	magnetic fluid
n	number of magnetic particles per unit volume (m^{-3})
N	frequency of revolutions / s
o	bearing center
O	journal center
p	fluid pressure in the film region (N m^{-2})
P	dimensionless film pressure defined in equation (6.22) for static case
\bar{P}	dimensionless film pressure defined in equation (6.46) for dynamic case

$\mathbf{q}=(u, v, w)$ fluid velocity vector, where u, v, w are components of the fluid in the x, y and z – directions, respectively

R_B bearing radius (m)

R_J journal radius (m)

S Sommerfeld number

\mathbf{S} internal angular momentum ($\text{K m}^2 \text{s}^{-1}$)

t time (s)

T temperature ($^\circ\text{K}$)

R, T radial and tangential co-ordinates (m)

R_1, T_1 radial and tangential co-ordinates (m)

$\hat{\mathbf{R}}, \hat{\mathbf{T}}$ unit vectors along the R, T – axis, respectively

$\hat{\mathbf{R}}_1, \hat{\mathbf{T}}_1$ unit vectors along the R_1, T_1 – axis, respectively

U, W velocities of the journal in the x and z – directions, respectively (m s^{-1})

W load-carrying capacity defined in equation (6.38) (N)

\bar{W} dimensionless load-carrying capacity defined in equation (6.39)

x, y, z Cartesian co-ordinates (m)

w.r.t. with respect to

Greek symbols

$\varepsilon = e / c$ bearing eccentricity ratio ($0 \leq \varepsilon \leq 1$)

μ_0 permeability of free space (N A^{-2})

η viscosity of the suspension (N s m^{-2})

$\eta = \eta_0(1 + \frac{5}{2}\phi)$ Einstein viscosity relation

η_0 viscosity of the carrier liquid (N s m^{-2})

θ	angular coordinate related to a fixed direction Θ
ξ	Langevin's parameter which is a measure of dimensionless field strength
φ	volume concentration of the particles
ϕ	attitude angle
τ_B	Brownian relaxation time (Brownian rotational diffusion time) (s)
τ_s	magnetic moment relaxation time (s)
ψ	instantaneous load direction
$\omega = 2\pi N$	angular (or rotational) velocity of the journal (rot s ⁻¹)
$\mathbf{\Omega} = \frac{1}{2}\nabla \times \mathbf{v}$	local angular velocity of rotation of the fluid (rad s ⁻¹)

6.1 INTRODUCTION

Journal bearings consist of a shaft which rotates freely in a metal sleeve, known as bearing surface. The shaft and metal sleeve are separated by thin film of lubricant. It is used widely as indispensable bearings in industry because of superior vibration absorption quality, shock resistance, long life, low wear and good damping characteristics, for example, they are used in internal combustion engines, centrifugal pumps etc.

Nada and Osman [1] studied Magnetic fluid (MF) lubricated finite hydrodynamic journal bearings using couple stress effect. The modified Reynolds equation is solved for different bearing characteristics. The results indicate the significant influence of couple stresses and magnetic effects on the bearing characteristics. Hsu *et. al.* [2] investigated long journal bearing for the combined effects of stochastic surface roughness using Ferrofluid (FF) lubricant. They showed that transverse and longitudinal roughnesses have opposite effects on the bearing characteristics. Hu and Xu [3] studied journal bearing using cohesion forces & couple stresses of MFs, and the effect of squeeze dynamics. The results show that dimensionless load-carrying capacity increases while friction coefficient decreases with the increase of squeeze parameter, cohesion force coefficient and couple stress parameter of the MF. Bhat *et. al.* [4] made comparative study of journal bearing with the use of conventional engine oil, FF and MR fluid as lubricant. The results show that frictional forces at the bearing surface are much higher when lubricated with magnetized MR fluid as compared to conventional oil.

The static and dynamic performances of FF lubricated long journal bearing using Shliomis model have been studied in this Chapter. The transverse uniform magnetic field is considered in this study. Modified Reynolds equation is derived using equation of continuity. For static case, dimensionless expressions for load-carrying capacity, frictional force and

coefficient of friction are studied. For dynamic case, dimensionless expressions for stiffness and damping coefficients are studied.

6.2 ANALYSIS

The schematic diagram of the impermeable journal bearing with center o and radius R_B , where journal is having center O and radius R_J , is shown in Figure 6.1. Here, the bearing surface is stationary. Let the x and z – axis is along the circumference of the bearing at A and perpendicular to it, respectively. Let $\hat{\mathbf{i}}$ and $\hat{\mathbf{k}}$ be the unit vectors along the x – axis and z – axis, respectively. Here, the journal bearing is lubricated with FF lubricant, whose flow behaviour is given by Shliomis model [5]. Let U and W be the velocities of the journal in the x and z – directions, respectively. The perpendicular distance between the journal surface and bearing surface is known as film thickness $h = h(x, t)$ and is given by the approximate expression

$$h = c + e \cos \theta = c(1 + \varepsilon \cos \theta) = c[1 + \varepsilon \cos \{\Theta - (\phi + \psi)\}]; \varepsilon = e/c, \quad (6.1)$$

where c is the radial clearance, e is the eccentricity, θ is the angular coordinate related to a fixed direction Θ through the attitude angle ϕ and the instantaneous load direction ψ , and ε ($0 \leq \varepsilon \leq 1$) is the bearing eccentricity ratio.

Assuming steady flow, neglecting inertia and the second derivative of the internal angular momentum \mathbf{S} , the basic FF flow equations using Shliomis model [1,6,7] are as follows.

Equation of motion

$$-\nabla p + \eta \nabla^2 \mathbf{q} + \mu_0 (\mathbf{M} \cdot \nabla) \mathbf{H} + \frac{\mu_0}{2} \nabla \times (\mathbf{M} \times \mathbf{H}) = \mathbf{0} \quad (6.2)$$

Equation of magnetization for a strong magnetic field

$$\mathbf{M} = \frac{M_0}{|\mathbf{H}|} (\mathbf{H} + \bar{\tau} \boldsymbol{\Omega} \times \mathbf{H}); \quad \bar{\tau} = \frac{\tau_B}{1 + \frac{\mu_0 \tau_B \tau_s M_0 |\mathbf{H}|}{I}} \quad (6.3)$$

Equation of continuity

$$\nabla \cdot \mathbf{q} = 0 \quad (6.4)$$

Maxwell's equations

$$\nabla \times \mathbf{H} = \mathbf{0} \quad (6.5)$$

$$\nabla \cdot (\mathbf{M} + \mathbf{H}) = 0 \quad (6.6)$$

where p is the fluid pressure in the film region, η is the viscosity of the suspension, $\mathbf{q} = (u, v, w)$ is the fluid velocity vector, μ_0 is the permeability of the free space, \mathbf{M} is the magnetization vector, \mathbf{H} is the applied magnetic field vector, M_0 is the equilibrium magnetization, $|\mathbf{H}|$ is magnetic field strength, $\boldsymbol{\Omega} = \frac{1}{2} \nabla \times \mathbf{q}$ is the local angular velocity of rotation of the fluid, τ_B is the Brownian relaxation time, τ_s is the magnetic moment relaxation time and I is the sum of moments of inertia of the particles per unit volume.

For an axially symmetric flow under a uniform magnetic field $\mathbf{H} = (0, 0, H_0)$ and defining the following quantities for a suspension of spherical particles [6, 7]

$$M_0 = nm(\coth \xi - \frac{1}{\xi}), \quad \xi = \frac{\mu m |\mathbf{H}|}{k_B T}, \quad \tau_B = \frac{3\eta V}{k_B T}, \quad V = \frac{\varphi}{n}, \quad \tau_s = \frac{I}{6\eta\varphi}, \quad (6.7)$$

equations (6.2), (6.3) yields

$$\frac{\partial^2 u}{\partial z^2} = \frac{1}{\eta_0 \left(1 + \frac{5}{2} \varphi\right) (1 + \tau)} \frac{\partial p}{\partial x}, \quad (6.8)$$

where

$$\tau = \frac{3}{2} \varphi \frac{\xi - \tanh \xi}{\xi + \tanh \xi}, \quad (6.9)$$

n is number of magnetic particles per unit volume, m is magnetic moment of a particle, k_B is the Boltzmann's constant, T is the temperature, φ is the volume concentration of the

particles, ξ is Langevin's parameter which is a measure of dimensionless field strength and $\eta = \eta_0(1 + \frac{5}{2}\varphi)$ (η_0 is the viscosity of the carrier liquid) is the Einstein viscosity relation.

Solving equation (6.8) for u using no-slip boundary conditions

$$u = 0 \text{ when } z = 0 \text{ and } u = U \text{ when } z = h \quad (6.10)$$

yields

$$u = \frac{z^2 - hz}{2\eta_0 \left(1 + \frac{5}{2}\varphi\right) (1 + \tau)} \frac{\partial p}{\partial x} + \frac{Uz}{h}. \quad (6.11)$$

Substituting equation (6.11) into the integral form of continuity equation (6.4) and integrated across the film thickness (0, h), yields

$$\frac{\partial}{\partial x} \left[\frac{h^3}{\eta_0 \left(1 + \frac{5}{2}\varphi\right) (1 + \tau)} \frac{\partial p}{\partial x} \right] = \underbrace{6h \frac{\partial U}{\partial x} - 6U \frac{\partial h}{\partial x}}_{\text{Due to wedge effect}} + \underbrace{12 \frac{\partial h}{\partial t}}_{\text{Due to squeeze effect}} \quad (6.13)$$

using Leibnitz's rule, $w_0 = 0$ (because bearing surface is stationary and impermeable), and squeeze velocity of the journal $W = \partial h / \partial t$ (where t is time).

Decomposing velocities U and W in terms of rotation and translation yields

$$U = U_r + U_t, \quad W = W_r + W_t, \quad (6.14)$$

respectively. The direction of components U_r , U_t and W_t are shown in figure 6.1 at B .

For Journal bearings [8]

$$\frac{U_t}{U_r} = O(10^{-3}) \quad (6.15)$$

and so

$$U \approx U_r \text{ and } W \approx W_t + U \frac{\partial h}{\partial x}, \quad (6.16)$$

referring figure 6.1.

Using equation (6.16), equation (6.13) becomes

$$\frac{\partial}{\partial x} \left[\frac{h^3}{\eta_0 \left(1 + \frac{5}{2} \phi\right) (1 + \tau)} \frac{\partial p}{\partial x} \right] = 6 \frac{\partial}{\partial x} (hU) + 12 \frac{\partial h}{\partial t}. \quad (6.17)$$

When journal is rotated with an angular velocity ω , then the position of the journal is moved to new position, say in (R, T) coordinate system centered at O (having unit vectors $\hat{\mathbf{R}}$ and $\hat{\mathbf{T}}$, respectively) as shown in figure 6.1. Due to this movement, there is an existence of components of translational velocities \dot{e} and $e(\dot{\phi} + \dot{\psi})$ measured along the line of centers \overline{oO} and perpendicular to it, respectively. Then the components of the translational velocity of the journal in the x and z – directions related with the components of the translational velocity as defined above (\dot{e} and $e(\dot{\phi} + \dot{\psi})$, respectively) by

$$U_t = \dot{e} \sin \theta - e(\dot{\phi} + \dot{\psi}) \cos \theta, W_t = \dot{e} \cos \theta + e(\dot{\phi} + \dot{\psi}) \sin \theta. \quad (6.18)$$

Using equations (6.1), (6.14) and (6.18), the first term of right hand side of equation (6.17) becomes

$$\begin{aligned} 6 \frac{\partial}{\partial x} (hU) &= 6 \frac{\partial}{\partial x} [h(U_r + U_t)] \\ &= 6 \frac{\partial}{\partial x} \left[hU_r \left(1 + \frac{U_t}{U_r}\right) \right] \\ &= 6 \frac{\partial}{\partial x} \left[hR_j \omega \left\{ 1 + \frac{c}{R_j} \left(\frac{\dot{e}}{\omega} \sin \theta - \varepsilon \frac{\dot{\phi} + \dot{\psi}}{\omega} \cos \theta \right) \right\} \right] \\ &\approx 6R_j \omega \frac{\partial h}{\partial x}, \end{aligned} \quad (6.19)$$

which is good to order c/R_j , provided that \dot{e} , $\dot{\phi}$ and $\dot{\psi}$ are all of order ω or smaller.

Therefore, equation (6.17), using equations (6.1) and (6.19), becomes

$$\frac{\partial}{\partial x} \left[\frac{h^3}{\eta_0 \left(1 + \frac{5}{2} \varphi\right) (1 + \tau)} \frac{\partial p}{\partial x} \right] = 6R_j \omega \frac{\partial h}{\partial x} + 12[\dot{e} \cos \theta + e(\dot{\phi} + \dot{\psi}) \sin \theta], \quad (6.20)$$

which is the modified Reynolds equation for the present study. This equation can be used for the study of both static ($\dot{e} = 0, \dot{\phi} = 0, \dot{\psi} = 0$) and dynamic ($\dot{e} \neq 0, \dot{\phi} \neq 0, \dot{\psi} \neq 0$) performances of the bearings as discussed below.

6.3 STATIC PERFORMANCE

In this case Reynolds equation (6.20) becomes

$$\frac{\partial}{\partial x} \left(h^3 \frac{\partial p}{\partial x} \right) = 6\eta_0 \left(1 + \frac{5}{2} \varphi\right) (1 + \tau) R_j \omega \frac{\partial h}{\partial x}. \quad (6.21)$$

Introducing the dimensionless quantities

$$\theta = \frac{x}{R_j}, \quad H = \frac{h}{c}, \quad P = \frac{p}{\eta_0 N \left(\frac{R_j}{c}\right)^2}, \quad (6.22)$$

equation (6.21), because of constant uniform transverse magnetic field and under the assumption of constant viscosity, reduces to

$$\frac{d}{d\theta} \left(H^3 \frac{dP}{d\theta} \right) = 12\pi \left(1 + \frac{5}{2} \varphi\right) (1 + \tau) \frac{dH}{d\theta}, \quad (6.23)$$

where $\omega = 2\pi N$ (N is frequency of revolutions / s), H is the dimensionless film thickness and P is the dimensionless film pressure.

Solving equation (6.23) for P using Sommerfeld boundary conditions with zero ambient pressure

$$P = 0 \text{ when } \theta = 0 \text{ and } P = 0 \text{ when } \theta = 2\pi \quad (6.24)$$

yields

$$P = 12\pi \left(1 + \frac{5}{2}\varphi\right) (1 + \tau) \left[\int_0^\theta \frac{1}{H^2} d\theta - \frac{\left(\int_0^{2\pi} \frac{1}{H^2} d\theta \right)}{\left(\int_0^{2\pi} \frac{1}{H^3} d\theta \right)} \int_0^\theta \frac{1}{H^3} d\theta \right]. \quad (6.25)$$

Using Sommerfeld variable transform [9, 10]

$$1 + \varepsilon \cos \theta = \frac{1 - \varepsilon^2}{1 - \varepsilon \cos \gamma} \quad (6.26)$$

Therefore, using equations (6.1), (6.22), and (6.26),

$$\int \frac{1}{H} d\theta = \frac{\gamma}{(1 - \varepsilon^2)^{1/2}} \quad (6.27)$$

$$\int \frac{1}{H^2} d\theta = \frac{1}{(1 - \varepsilon^2)^{3/2}} (\gamma - \varepsilon \sin \gamma) \quad (6.28)$$

and

$$\int \frac{1}{H^3} d\theta = \frac{1}{(1 - \varepsilon^2)^{5/2}} \left(\gamma - 2\varepsilon \sin \gamma + \frac{\varepsilon^2 \gamma}{2} + \frac{\varepsilon^2 \sin 2\gamma}{4} \right). \quad (6.29)$$

Using equation (6.26), the boundaries

$$\theta = 0 \Rightarrow \gamma = 0 \text{ and } \theta = 2\pi \Rightarrow \gamma = 2\pi.$$

Therefore, using equations (6.27) - (6.29),

$$\int_0^{2\pi} \frac{1}{H} d\theta = \frac{2\pi}{(1 - \varepsilon^2)^{1/2}} \quad (6.30)$$

$$\int_0^{2\pi} \frac{1}{H^2} d\theta = \frac{2\pi}{(1 - \varepsilon^2)^{3/2}} \quad (6.31)$$

and

$$\int_0^{2\pi} \frac{1}{H^3} d\theta = \frac{(2 + \varepsilon^2)\pi}{(1 - \varepsilon^2)^{5/2}}. \quad (6.32)$$

Using equations (6.28), (6.29), (6.31), (6.32), (6.25) becomes

$$P = \frac{12\pi \left(1 + \frac{5}{2}\varphi\right) (1 + \tau)\varepsilon \sin \gamma (2 - \varepsilon^2 - \varepsilon \cos \gamma)}{(2 + \varepsilon^2)(1 - \varepsilon^2)^{3/2}}. \quad (6.33)$$

Using equation (6.26),

$$\cos \gamma = \frac{\varepsilon + \cos \theta}{1 + \varepsilon \cos \theta} \quad \text{and} \quad \sin \gamma = \frac{(1 - \varepsilon^2)^{1/2} \sin \theta}{1 + \varepsilon \cos \theta}, \quad (6.34)$$

therefore, equation (6.33) in terms of original variable θ becomes

$$P = \frac{12\pi \left(1 + \frac{5}{2}\varphi\right) (1 + \tau)\varepsilon \sin \theta (2 + \varepsilon \cos \theta)}{(2 + \varepsilon^2)(1 + \varepsilon \cos \theta)^2}. \quad (6.35)$$

Using equations (6.1), (6.22) and (6.25), the dimensionless form of radial component of fluid film force is

$$f_R = \frac{1}{2} \int_0^{2\pi} P \cos \theta d\theta = 0. \quad (6.36)$$

Similarly, using equations (6.1), (6.22), (6.25), (6.27) – (6.32), the dimensionless form of tangential component of fluid film force is

$$f_T = \frac{1}{2} \int_0^{2\pi} P \sin \theta d\theta = \frac{12\pi^2 \left(1 + \frac{5}{2}\varphi\right) (1 + \tau)\varepsilon}{(2 + \varepsilon^2)(1 - \varepsilon^2)^{1/2}} = \frac{1}{S}, \quad (6.37)$$

where S is Sommerfeld number.

6.3.1 CALCULATION OF BEARING CHARACTERISTICS

(a) *Load-carrying capacity* The load-carrying capacity is given by

$$W = LD_J \eta_0 N \left(\frac{R_J}{c}\right)^2 (f_R^2 + f_T^2)^{1/2}, \quad (6.38)$$

where D_J is the journal diameter and L length of the bearing in the y – direction.

Using equations (6.36) and (6.37), the dimensionless form of W becomes

$$\bar{W} = \frac{W}{LD_J \eta_0 N \left(\frac{R_J}{c} \right)^2} = \frac{12\pi^2 \left(1 + \frac{5}{2} \phi \right) (1 + \tau) \varepsilon}{(2 + \varepsilon^2)(1 - \varepsilon^2)^{1/2}}. \quad (6.39)$$

(b) *Frictional Force on the Journal* The frictional force on the journal is given by

$$F = \int_{-L/2}^{L/2} \int_0^{2\pi R_J} \eta \frac{\partial u}{\partial z} \Big|_{z=h} dx dy. \quad (6.40)$$

Using equations (6.1), (6.11), (6.22), (6.30), (6.37), $\omega = 2\pi N$ and $U = R_J \omega$, the dimensionless form of F becomes

$$\bar{F} = \frac{cF}{\eta_0 L N R_J D_J} = \left(1 + \frac{5}{2} \phi \right) \frac{4\pi^2 (1 + 2\varepsilon^2)}{(2 + \varepsilon^2)(1 - \varepsilon^2)^{1/2}}. \quad (6.41)$$

(c) *Coefficient of Friction on the Journal* The coefficient of friction on the journal in dimensionless form is given by

$$\bar{f} = \frac{\bar{F}}{\bar{W}} = \frac{1 + 2\varepsilon^2}{3\varepsilon(1 + \tau)}. \quad (6.42)$$

6.4 DYNAMIC PERFORMANCE

Due to rotation of the journal, there is an existence of residual imbalance and due to this the journal center is not confined to a point but moves along some locus. Thus, the orbit frequency, amplitude, operating conditions, fluid-film characteristics, etc. determines the dynamic behaviour of the bearing system.

In general, due to squeeze velocity and lubricant forces (or there is a small unbalanced force on the journal) $\dot{e} \neq 0, \dot{\phi} \neq 0, \dot{\psi} \neq 0$, the position of the journal is moved from its position in (R, T) coordinate system centered at O (as mentioned above) to new instantaneous position, say in (R_1, T_1) coordinate system centered at O_N (having unit vectors $\hat{\mathbf{R}}_1$ and $\hat{\mathbf{T}}_1$, respectively) as shown in figure 6.2 (which is continuation of figure 6.1). Due to

this new position, there is change in eccentricity from e to $e_N = e + \Delta e$ and attitude angle from ϕ to $\phi_N = \phi + \Delta\phi$. Moreover, the components of the lubricant forces in radial direction f_R and tangential direction f_T in coordinate system (R, T) is related with the components of the lubricant forces in radial direction f_{R_1} and tangential direction f_{T_1} in new coordinate system (R_1, T_1) by

$$\left. \begin{aligned} f_R &= (\cos \Delta\phi) f_{R_1} + [\cos(\frac{\pi}{2} + \Delta\phi)] f_{T_1} = (\cos \Delta\phi) f_{R_1} - (\sin \Delta\phi) f_{T_1} \\ f_T &= [\cos(\frac{3\pi}{2} + \Delta\phi)] f_{R_1} + (\cos \Delta\phi) f_{T_1} = (\sin \Delta\phi) f_{R_1} + (\cos \Delta\phi) f_{T_1} \end{aligned} \right\} \quad (6.43)$$

If $\Delta\phi \rightarrow 0$, then the increase in force components Δf_R and Δf_T becomes

$$\left. \begin{aligned} \Delta f_R &= f_{R_1} - \Delta\phi f_{T_1} - f_R \\ \Delta f_T &= \Delta\phi f_{R_1} + f_{T_1} - f_T \end{aligned} \right\} \quad (6.44)$$

Using Taylor series expansion for f_{R_1} and f_{T_1} about static equilibrium position and neglecting higher-order terms, yields

$$\begin{bmatrix} df_R \\ df_T \end{bmatrix} = \begin{bmatrix} \frac{\partial f_R}{\partial e} & \frac{\partial f_R}{\partial \phi} - f_T \\ \frac{\partial f_T}{\partial e} & \frac{\partial f_T}{\partial \phi} + f_R \end{bmatrix} \begin{bmatrix} de \\ d\phi \end{bmatrix} + \begin{bmatrix} \frac{\partial f_R}{\partial \dot{e}} & \frac{\partial f_R}{\partial \dot{\phi}} \\ \frac{\partial f_T}{\partial \dot{e}} & \frac{\partial f_T}{\partial \dot{\phi}} \end{bmatrix} \begin{bmatrix} d\dot{e} \\ d\dot{\phi} \end{bmatrix}. \quad (6.45)$$

Equation (6.20) with the dimensionless quantities

$$\theta = \frac{x}{R_J}, \quad H = \frac{h}{c}, \quad \bar{P} = \frac{P}{\eta_0 N \left(\frac{R_J}{c}\right)^2 \left(1 - \frac{2\dot{\phi}}{\omega}\right)} \quad (6.46)$$

becomes

$$\frac{\partial}{\partial \theta} \left[H^3 \frac{\partial \bar{P}}{\partial \theta} \right] = \left(1 + \frac{5}{2} \varphi\right) (1 + \tau) \left[-12\pi\epsilon \sin \theta + \frac{24\pi\dot{\epsilon}}{\omega \left(1 - \frac{2\dot{\phi}}{\omega}\right)} \cos \theta \right], \quad (6.47)$$

using equation (6.1), $\omega = 2\pi N$, constant uniform transverse magnetic field and under the assumption of constant viscosity, considering only the radial component (that is, component

in the direction of \overline{oO}), and neglecting $2\dot{\phi}/\omega$ for wedge effect since for wedge effect more concentration is given on rotational velocity of the journal rather than whirling motion of the journal.

Solving equation (6.47) for \bar{P} using Sommerfeld boundary conditions with zero ambient pressure

$$\bar{P} = 0 \text{ when } \theta = 0 \text{ and } \bar{P} = 0 \text{ when } \theta = 2\pi \quad (6.48)$$

yields

$$\bar{P} = \left(1 + \frac{5}{2}\varphi\right)(1 + \tau) \left[12\pi \left\{ \int_0^\theta \frac{1}{H^2} d\theta - \frac{\int_0^{2\pi} \frac{1}{H^2} d\theta}{\int_0^{2\pi} \frac{1}{H^3} d\theta} \int_0^\theta \frac{1}{H^3} d\theta \right\} + 24\pi \left(\frac{\frac{\dot{\varepsilon}}{\omega}}{1 - \frac{2\dot{\phi}}{\omega}} \int_0^\theta \frac{\sin \theta}{H^3} d\theta \right) \right] \quad (6.49)$$

using equations (6.1) and (6.46).

Using equations (6.28), (6.29), (6.31), (6.32), (6.34) and referring [10], equation (6.49) becomes

$$\bar{P} = 12\pi \left(1 + \frac{5}{2}\varphi\right)(1 + \tau) \left[\frac{\varepsilon \sin \theta (2 + \varepsilon \cos \theta)}{(2 + \varepsilon^2)(1 + \varepsilon \cos \theta)^2} + \frac{1}{\varepsilon} \left\{ \frac{1}{(1 + \varepsilon \cos \theta)^2} - \frac{1}{(1 + \varepsilon)^2} \right\} \left(\frac{\frac{\dot{\varepsilon}}{\omega}}{1 - \frac{2\dot{\phi}}{\omega}} \right) \right]. \quad (6.50)$$

Using equations (6.1), (6.30)-(6.32) and (6.50), the dimensionless form of radial component of fluid film force is

$$f_{R_1} = \frac{1}{2} \int_0^{2\pi} \bar{P} \cos \theta d\theta = - \frac{12\pi^2 \left(1 + \frac{5}{2}\varphi\right)(1 + \tau)}{(1 - \varepsilon^2)^{3/2}} \left(\frac{\frac{\dot{\varepsilon}}{\omega}}{1 - \frac{2\dot{\phi}}{\omega}} \right). \quad (6.51)$$

Similarly, using equations (6.1), (6.30) - (6.32), (6.46), (6.50) and referring [10], the dimensionless form of tangential component of fluid film force is

$$f_{T_1} = \frac{1}{2} \int_0^{2\pi} \bar{P} \sin \theta d\theta = \frac{12\pi^2 \left(1 + \frac{5}{2}\varphi\right)(1+\tau)\varepsilon}{(2+\varepsilon^2)(1-\varepsilon^2)^{1/2}}. \quad (6.52)$$

6.4.1 CALCULATION OF THE DIMENSIONLESS STIFFNESS MATRIX K AND DAMPING MATRIX C

According to [8], and using equations (6.45), (6.51), (6.52), the dimensionless form of the stiffness matrix K and damping matrix C are given by

$$K = \begin{bmatrix} K_{R_1R_1} & K_{R_1T_1} \\ K_{T_1R_1} & K_{T_1T_1} \end{bmatrix} = \begin{bmatrix} \frac{\partial f_{R_1}}{\partial \varepsilon} & \frac{\partial f_{R_1}}{\varepsilon \partial \phi} - \frac{f_{T_1}}{\varepsilon} \\ \frac{\partial f_{T_1}}{\partial \varepsilon} & \frac{\partial f_{T_1}}{\varepsilon \partial \phi} + \frac{f_{R_1}}{\varepsilon} \end{bmatrix} \quad (6.53)$$

and

$$C = \begin{bmatrix} C_{R_1R_1} & C_{R_1T_1} \\ C_{T_1R_1} & C_{T_1T_1} \end{bmatrix} = \begin{bmatrix} \frac{\partial f_{R_1}}{\partial (\dot{\varepsilon}/\omega)} & -\frac{2f_{R_1}}{\varepsilon} \\ \frac{\partial f_{T_1}}{\partial (\dot{\varepsilon}/\omega)} & -\frac{2f_{T_1}}{\varepsilon} \end{bmatrix}, \quad (6.54)$$

respectively.

It should be noted that the above two matrices can be found out for all forces and their derivatives which are evaluated under the conditions of static equilibrium. Moreover, the rate of change of f_R with respect to $\dot{\varepsilon}/\omega$ can be evaluated at arbitrary value of $\dot{\phi}$ (say zero).

Using (6.51)-(6.54),

$$K = \begin{bmatrix} 0 & -\frac{12\pi^2 \left(1 + \frac{5}{2}\varphi\right)(1+\tau)}{(2+\varepsilon^2)(1-\varepsilon^2)^{1/2}} \\ \frac{12\pi^2 \left(1 + \frac{5}{2}\varphi\right)(1+\tau)(2-\varepsilon^2 + 2\varepsilon^4)}{(2+\varepsilon^2)^2(1-\varepsilon^2)^{3/2}} & 0 \end{bmatrix} \quad (6.55)$$

and

$$C = \begin{bmatrix} -\frac{12\pi^2 \left(1 + \frac{5}{2}\varphi\right)(1+\tau)}{(1-\varepsilon^2)^{3/2}} & 0 \\ 0 & -\frac{24\pi^2 \left(1 + \frac{5}{2}\varphi\right)(1+\tau)}{(2+\varepsilon^2)(1-\varepsilon^2)^{1/2}} \end{bmatrix}. \quad (6.56)$$

6.5 RESULTS AND DISCUSSION

The representative values of the different parameters taken in computations are as follows [11].

$$\pi = 22/7, \quad \varphi = 0.0075, \quad \mu_0 m = 1.75 \times 10^{-25} \text{ (J A}^{-1} \text{ m)},$$

$$|\mathbf{H}| = 10^5 \text{ (A m}^{-1}\text{)}, \quad k_B = 1.38 \times 10^{-23} \text{ J (}^\circ\text{K)}^{-1}, \quad T = 297 \text{ (}^\circ\text{K)},$$

Also, for smaller values of ξ ,

$$\tau = \frac{3}{2} \varphi \frac{\xi - \tanh \xi}{\xi + \tanh \xi} \rightarrow 0.$$

Effect of variation of the eccentricity ratio ε ($0 < \varepsilon < 1$) on different dimensionless bearing characteristics for static and dynamic cases, is shown in figures 6.3-6.9.

Case 1: Effect of FF lubricant with an applied transverse magnetic field: $\varphi = 0.0075$, $\tau = 0.006981701344650$ (which indicates the effects of volume concentration of the magnetic particles in the magnetic suspension as well as applied magnetic field on FF)

Case 2: Effect of conventional lubricant: $\varphi = 0.0$, $\tau = 0.0$ (which indicates no effects of volume concentration of the magnetic particles in the magnetic suspension as well as no applied magnetic field on FF)

Case 3: Effect of FF lubricant without applied magnetic field: $\varphi = 0.0075$, $\tau = 0.0$ (which indicates the effects of volume concentration of the magnetic particles in the magnetic suspension without applied magnetic field – the case of FF lubricant without magnetic field effect)

Figure 6.3 shows the variation in dimensionless load-carrying capacity \bar{W} against the variation in the eccentricity ratio ε for both Case 1 (solid line) and Case 2 (dotted line). In general, it is observed that with the increasing value of ε from 0.1 to 0.9, \bar{W} increases for both the Case 1 and Case 2 but because of FF as lubricant \bar{W} increase significantly (Case 1) than conventional lubricant (Case 2). Moreover, as compared to conventional lubricant, the growth rate of \bar{W} is continuously increasing with the increasing values of ε from 0.1 to 0.9. This behaviour of \bar{W} is in contrast to the behaviour obtained in [12], in which, with the increasing values of ε from 0.1 to 0.9, the effect of FF on \bar{W} is reduced and become zero when $\varepsilon \approx 0.6$.

Figure 6.4 shows the variation in dimensionless frictional force \bar{F} against the variation of eccentricity ratio ε . It is observed from the expression (equation (6.41)) of \bar{F} that there is no effect of magnetic field parameter τ on \bar{F} . In this figure, there are two curves – one for $\varphi = 0.0075$ (solid line) and second for $\varphi = 0.0$ (dotted line). It shows, in general, that with the increasing value of ε , \bar{F} increases. However, the increase in the values of \bar{F} is negligible for FF lubricant which may be due to slightly increase in the viscosity of FF lubricant than conventional lubricant.

Figure 6.5 shows the variation in dimensionless coefficient of friction \bar{f} against the variation of eccentricity ratio ε . Two curves – one for $\tau = 0.006981701344650$ (solid line)

and second for $\tau = 0$ (dotted line) are shown in this figure. In general, it is observed that \bar{f} decreases with the increasing values of ε . Moreover, the behaviour of \bar{f} is almost same for both the curve as the two curves almost coincide over each other.

The variation in dimensionless stiffness coefficients $-K_{R_1T_1}$ and $K_{T_1R_1}$ for different values of eccentricity ratio ε is shown in figures 6.6 and 6.7, respectively, for Case 1 (solid line) and Case 2 (dotted line). It is observed, in general, that both $-K_{R_1T_1}$ and $K_{T_1R_1}$ increases with the increasing values of ε . Moreover, the effect of FF lubricant is more significant when ε moves from 0.1 to 0.9 as compared to conventional lubricant.

Figures 6.8 and 6.9 shows the variation in dimensionless damping coefficient $-C_{R_1R_1}$ and $-C_{T_1T_1}$, respectively, for different values of eccentricity ratio ε for Case 1 (solid line) and Case 2 (dotted line). It is observed, in general, that both $-C_{R_1R_1}$ and $-C_{T_1T_1}$ increases with the increasing values of ε ; that means, $C_{R_1R_1}$ and $C_{T_1T_1}$ decreases with the increasing values of ε . It is also observed that effect of FF lubricant is more significant when ε moves from 0.1 to 0.9 as compared to conventional lubricant.

6.6 CONCLUSIONS

This chapter deals with the study of static and dynamic performances of FF lubricated long journal bearing. Using equation of motion of FF given by Shliomis [5] and equation of continuity, modified Reynolds equation is derived. The dimensionless expressions for load-carrying capacity (\bar{W}), frictional force (\bar{F}) and coefficient of friction (\bar{f}) are studied for static case, while the dimensionless expressions for stiffness coefficients ($-K_{R_1T_1}$ and $K_{T_1R_1}$) and damping coefficients ($-C_{R_1R_1}$ and $-C_{T_1T_1}$) are studied for dynamic case.

The results conclude the following.

1. \bar{W} increases with the increasing values of eccentricity ratio ε , and the effects of FF lubricant in the presence of magnetic field is more significant than conventional lubricant.
2. \bar{F} increases with the increasing values of ε . However, there is almost negligible difference between the values of \bar{F} for $\varphi = 0.0075$ and $\varphi = 0.0$.
3. \bar{f} decreases with the increasing values of ε , and the effects of FF lubricant in the presence of magnetic field is almost same as that of conventional lubricant.
4. All coefficients $-K_{R,T_1}$, K_{T,R_1} , $-C_{R,R_1}$ and $-C_{T,T_1}$ increases with the increasing values of ε .
In all cases effect of FF lubricant is more significant when ε moves from 0.1 to 0.9 as compared to conventional lubricant.

Thus, FF lubricant in the presence of a transverse uniform magnetic field leads to an added advantage of higher load-carrying capacity without significantly increases in the frictional force. Moreover, comparing with conventional lubricant the bearing performance is significantly modified with the use of FF lubricant.

REFERENCES

1. Nada GS, Osman TA. 2007 Static performance of finite hydrodynamic journal bearings lubricated by magnetic fluids with couple stresses. *Tribology Letters*, 27: 261-268.
2. Hsu TC, Chen JH, Chiang HL, Chou TL. 2014 Combined effects of magnetic field and surface roughness on long journal bearing lubricated with ferrofluid. *Journal of Marine Science and Technology*, 2(22): 154-162.
3. Hu R, Xu C. 2017 Influence of magnetic fluids' cohesion force and squeeze dynamic effect on the lubrication performance of journal bearing. *Advances in Mechanical Engineering*, 9(9): 1-13.
4. Bhat AK, Vaz N, Kumar Y, D'Silva R, Kumar P, Bindu KG. 2019 Comparative study of journal bearing performance with ferrofluid and MR fluid as lubricant. *AIP Conference Proceedings* 2080, 040008.
5. Shliomis MI. 1972 Effective viscosity of magnetic suspensions. *Soviet Physics JETP*, 34 (6): 1291–1294.
6. Shah RC, Bhat MV. 2005 Ferrofluid squeeze film between curved annular plates including rotation of magnetic particles. *Journal of Engineering Mathematics*, 51: 317-324.
7. Shah RC, Parikh KS. 2014 Comparative study of ferrofluid lubricated various designed slider bearings considering rotation of magnetic particles and squeeze velocity. *International Journal of Theoretical and Mathematical Physics*, 4(2): 63-72.
8. Szeri AZ. 2005 *Fluid Film Lubrication Theory & Design*. Cambridge University Press, UK.
9. Pinkus O, Sternlicht B. 1961 *Theory of Hydrodynamic Lubrication*. McGraw-hill, New York.
10. Hori Y. 2006 *Hydrodynamic Lubrication*. Springer-Verlag Tokyo.
11. Shah RC, Shah RB. 2018 Derivation of ferrofluid lubrication equation for slider bearings with variable magnetic field and rotations of the carrier liquid as well as magnetic particles. *Meccanica*, 53(4-5): 857-869.

12. Osman TA, Nada GS, Safar ZS. 2001 Static and dynamic characteristics of magnetized journal bearings lubricated with ferrofluid. *Tribology International*, 34(6): 369-380.

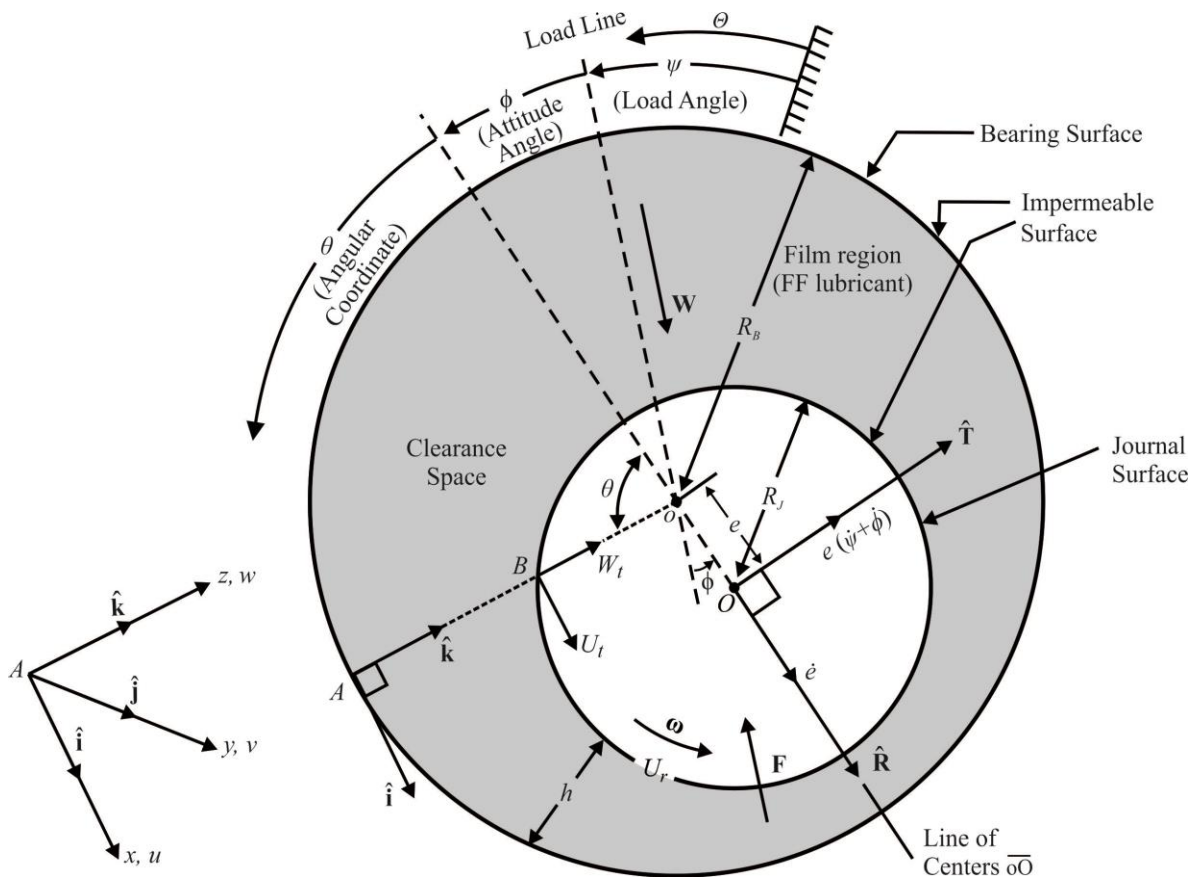


Figure 6.1 Journal bearing

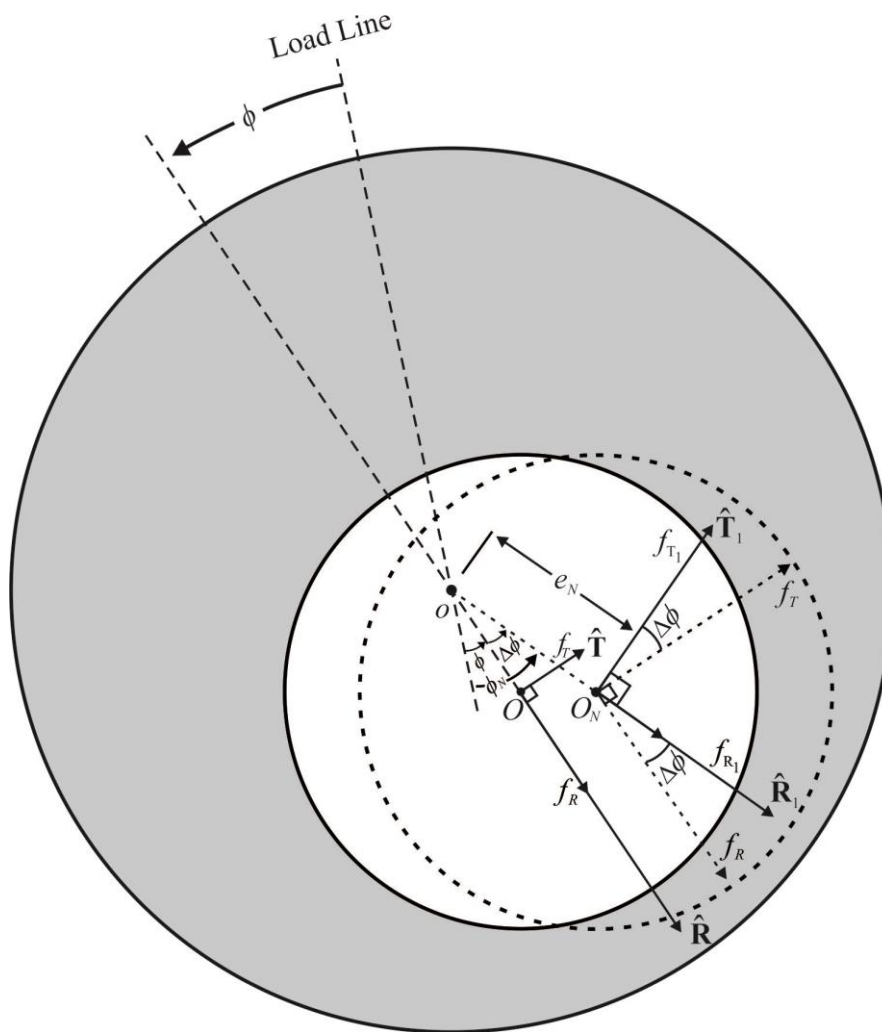


Figure 6.2 Force decomposition in Journal bearing (which is continuation of Figure 6.1)

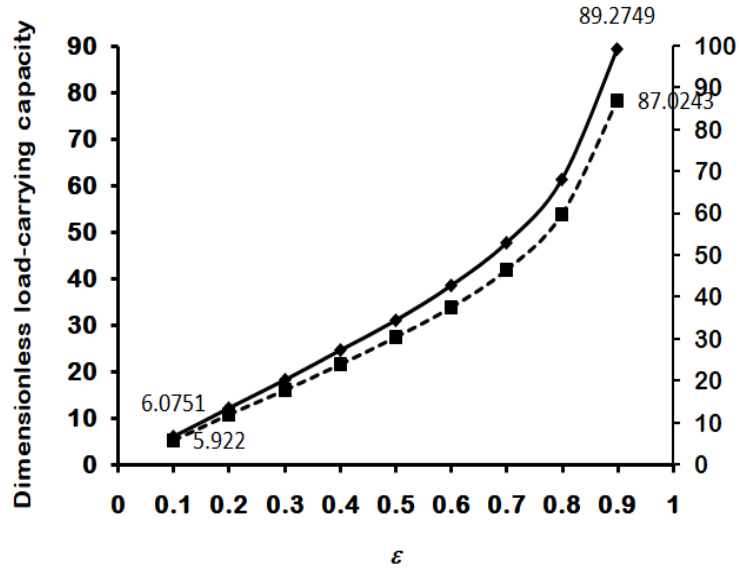


Figure 6.3 Variation in dimensionless load-carrying capacity \bar{W} for different values of eccentricity ratio ϵ for Case 1 (solid line) and Case 2 (dotted line)

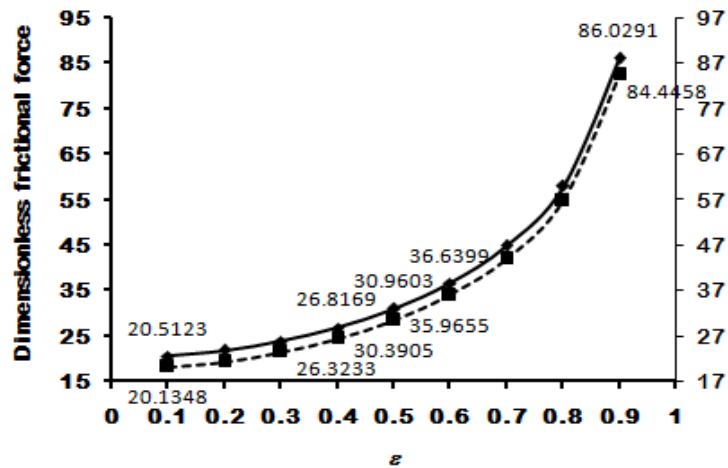


Figure 6.4 Variation in dimensionless frictional force \bar{F} for different values of eccentricity ratio ϵ for $\phi = 0.0075$ (solid line) and $\phi = 0.0$ (dotted line)

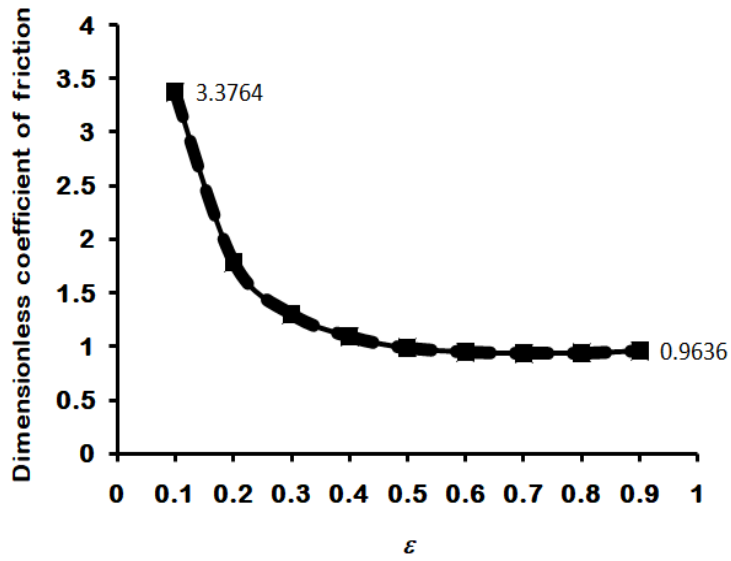


Figure 6.5 Variation in dimensionless coefficient of friction \bar{f} for different values of eccentricity ratio ε for $\tau = 0.006981701344650$ (solid line) and $\tau = 0$ (dotted line) considering $\varphi = 0.0075$

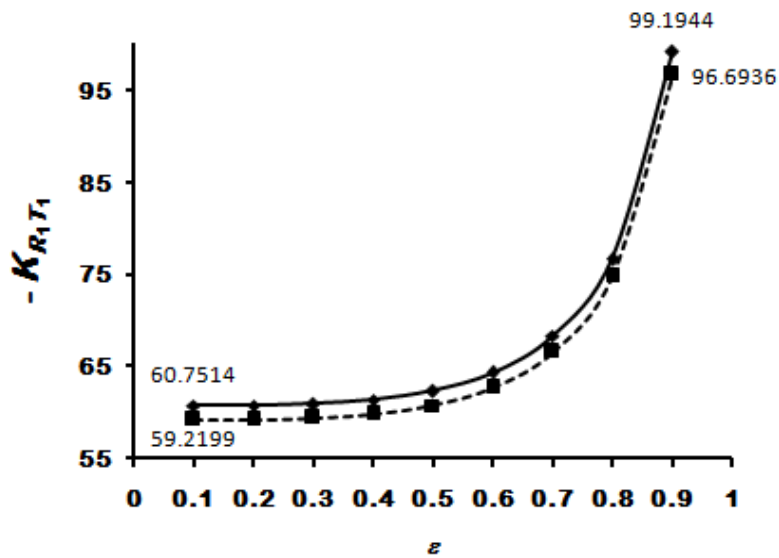


Figure 6.6 Variation in dimensionless stiffness coefficient $-K_{R,T_1}$ for different values of eccentricity ratio ε for Case 1 (solid line) and Case 2 (dotted line)

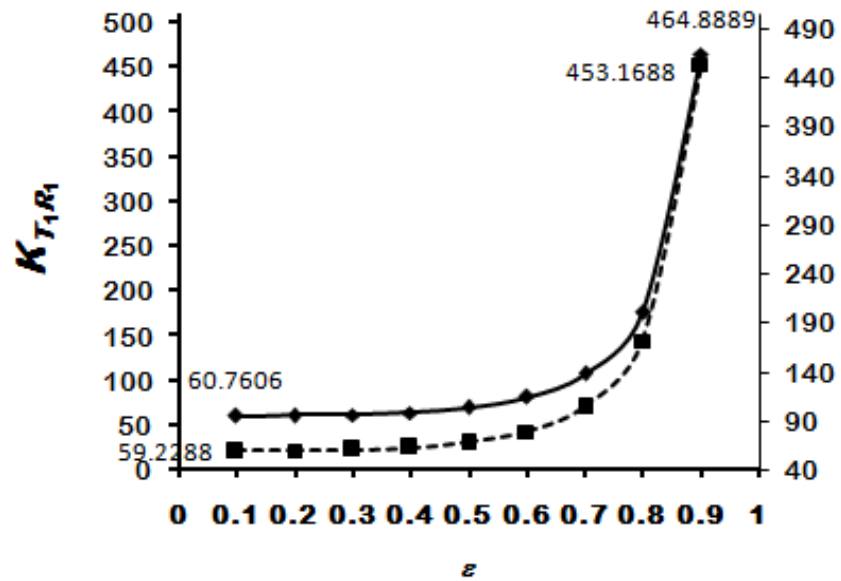


Figure 6.7 Variation in dimensionless stiffness coefficient $K_{T_1 R_1}$ for different values of eccentricity ratio ε for Case 1 (solid line) and Case 2 (dotted line)

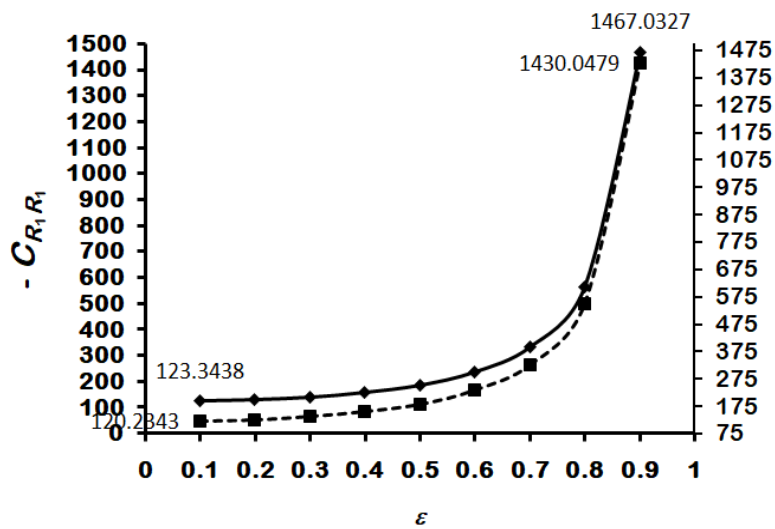


Figure 6.8 Variation in dimensionless damping coefficient $-C_{R_1 R_1}$ for different values of eccentricity ratio ε for Case 1 (solid line) and Case 2 (dotted line)

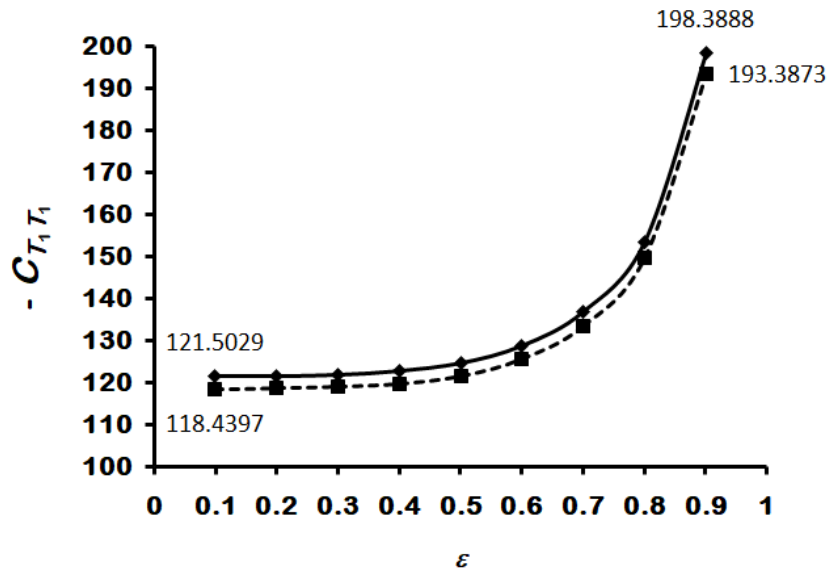


Figure 6.9 Variation in dimensionless damping coefficient $-C_{T_1 T_1}$ for different values of eccentricity ratio ϵ for Case 1 (solid line) and Case 2 (dotted line)